12266–12273 *Nucleic Acids Research, 2022, Vol. 50, No. 21* *Published online 1 December 2022*
https://doi.org/10.1093/nar/gkac1101

Human DNA polymerase α has a strong mutagenic potential at the initial steps of DNA synthesis

Alisa E. Lisova†, Andrey G. Baranovskiy†, Lucia M. Morstadt, Nigar D. Babayeva and Tahir H. Tahirov*

Eppley Institute for Research in Cancer and Allied Diseases, Fred & Pamela Buffett Cancer Center, University of Nebraska Medical Center, Omaha, NE 68198, USA

Received August 12, 2022; Revised September 16, 2022; Editorial Decision October 27, 2022; Accepted November 10, 2022

ABSTRACT

DNA polymerase α (Polα) is essential for DNA replication initiation and makes a notable contribution to genome mutagenesis. The activity and fidelity of Polα during the early steps of DNA replication have not been well studied. Here we show that at the beginning of DNA synthesis, when extending the RNA primer received from primase, Polα is more mutagenic than during the later DNA elongation steps. Kinetic and binding studies revealed substantially higher activity and affinity to the template:primer when Polα interacts with ribonucleotides of a chimeric RNA–DNA primer. Polα activity greatly varies during first six steps of DNA synthesis, and the bias in the rates of correct and incorrect dNTP incorporation leads to impaired fidelity, especially upon the second step of RNA primer extension. Furthermore, increased activity and stability of Polα/template:primer complexes containing RNA–DNA primers result in higher efficiency of mismatch extension.

INTRODUCTION

During replication of the eukaryotic genome at each cell division, DNA polymerase α (Polα) initiates DNA synthesis at the thousands of replication origins and on the millions of Okazaki fragments (1,2). In the tightly regulated primosome complex, Polα receives from primase the 9-mer RNA primer (3) for further extension with deoxynucleotides, which results in generation of a chimeric RNA–DNA primer with a length of ∼35 nucleotides (4,5) (Figure 1) essential for loading the main replicative DNA polymerases ε and δ. As other DNA polymerases (6), Polα binds two substrates, template:primer (T:P) and dNTP, and catalyzes the covalent attachment of a deoxynucleotide monophosphate (dNMP) to the primer 3′-end with a release of pyrophosphate. In addition to genome replication and telomere maintenance (7–10), Polα is involved in regulation of the interferon I response (11) and is a promising target for anti-tumor drugs like CD437 (12).

In contrast to other replicative DNA polymerases, Polα has a unique ability to efficiently work on RNA and DNA primers (13). Like the error-prone DNA polymerase ζ (14), Polα does not possess proofreading 3′-exonuclease activity, resulting in fidelity that is one order of magnitude lower compared to Polδ and Polε (15). Recently it was shown that the Polα-synthesized mutagenic DNA is retained in the mature genome despite the ability of Polδ and mismatch repair system to correct the Polα mistakes (16).

In spite of the important role of Polα in mutagenesis and evolution of eukaryotic genomes, Polα fidelity studies are sparse, lack high-resolution approaches, and are mainly focused on the late stage of DNA primer synthesis (17–22). In this work, we analyzed Polα fidelity at two main stages of DNA synthesis: the early DNA elongation stage when Polα extends the RNA primer with the first eight dNMPs (referred to as steps 1 to 8), and the following late stage when Polα interacts only with the DNA region of a RNA–DNA primer (Figure 1). We employed a single-turnover kinetic analysis and a real-time binding assay to estimate the effect of different mismatches (MMs) at the insertion and post-insertion sites of Polα on the rate of DNA polymerization and stability of the Polα/T:P complex. Together, these approaches allow for estimating the efficiencies of MM insertion and extension (Figure 2).

MATERIALS AND METHODS

Protein expression and purification

Cloning, expression, and purification to homogeneity of Polα catalytic domain have been described elsewhere (13). Peak fractions obtained from a Heparin HP HiTrap column (Cytiva) were combined and dialyzed to 25 mM Tris–HEPES, pH 7.8, 200 mM NaCl, 1% glycerol and 1 mM tris(2-carboxyethyl)phosphine (TCEP), concentrated

*To whom correspondence should be addressed. Tel: +1 402 559 7608; Fax: +1 402 559 3739; Email: ttahirov@unmc.edu
†The authors wish it to be known that, in their opinion, the first two authors should be regarded as Joint First Authors.

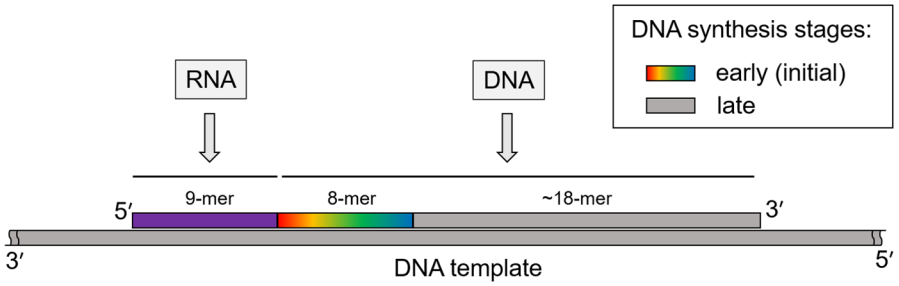

Figure 1. Structure of a mature RNA–DNA primer synthesized by primase-Polα (primosome) on a parental DNA template.

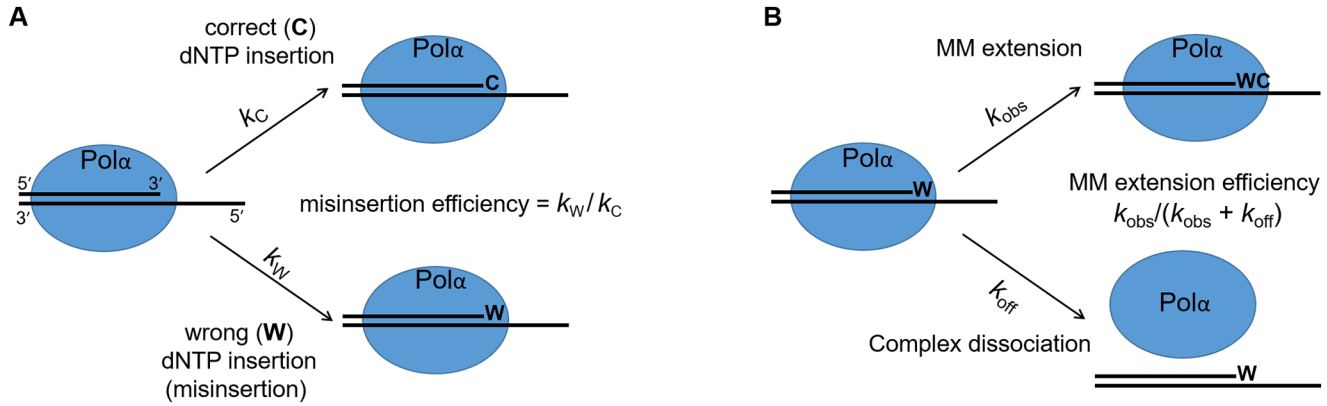

Figure 2. Experimental design. Schematics of experiments for estimation of misinsertion efficiency (**A**) and mismatch extension efficiency (**B**). k_c and k_w describe the rates of primer extension with correct (cognate) and wrong (non-cognate) nucleotide. k_{obs} and k_{off} describe the rate of primer extension and the rate of Polα/T:P complex dissociation, respectively.

to ∼100 μM and flash frozen in aliquots. Human primosome was obtained according to (23).

Binding studies

Analysis of binding kinetics was done at 23°C on an Octet K2 (Sartorius AG) as previously described (24). This device uses Bio-Layer Interferometry technology to monitor molecular interactions in real time. This allows for obtaining the rate constants of complex formation (k_{on}), dissociation (k_{off}), and the dissociation constant (K_D). The template with a biotin-TEG at the 5′-overhang was annealed to the primers (Supplemental Table S1) and immobilized on a streptavidin-coated biosensor (SAX, Sartorius AG). Primers were added at two-fold molar excess to the template. To prevent DNA polymerase reaction, a dideoxycytidine was placed at the 3-end of primers. SAX sensors were loaded with oligonucleotide-biotin at 50 nM concentration for 7 min at 500 rpm. Then sensors were blocked by incubating for 2 min in 10 μg/ml biocytin. In the first row of a 96-well microplate (Greiner Bio-One), the first six wells contained the buffer, consisting of 25 mM Tris-Hepes, pH 7.8, 150 mM KCl, 2 mM TCEP, and 0.002% Tween 20. The next six wells contained the two-fold dilutions of hPolα in the same buffer. When binding studies were performed in presence of an incoming nucleotide, 50 μM dNTP and 5 mM $MgCl_2$ were added to the buffer. All wells in the second row contained only the buffer for reference. Data Analysis HT software (version 11.1, Sartorius AG) was used for calculation of binding constants (k_{on}, k_{off} and K_D). The average value and standard deviation were calculated from three independent experiments.

Kinetic studies

Pre-steady-state kinetic studies were performed at single-turnover conditions on the QFM-4000 rapid chemical quench apparatus (BioLogic, France) at 35°C. Reactions contained 3 μM hPolα_{CD}, 0.25 μM duplex, varying concentrations of dNTP, 25 mM Tris–HEPES, pH 7.8, 0.15 M KCl, 5 mM $MgCl_2$, 2 mM TCEP and 0.2 mg/mL BSA. hPolα was incubated with a fluorescence-labeled 15-mer primer annealed to a 25-mer DNA template (Supplemental Table S1), to allow for the formation of the binary complex, and rapidly mixed with 10 μM dTTP and 5 mM $MgCl_2$ (final concentrations) followed by quenching with 0.3 M EDTA. Mismatch insertion kinetics were conducted in the presence of 50 μM dNTP to avoid prolonged incubation. Products were collected in a tube containing 17 μl 100% formamide and separated by denaturing urea PAGE. The fluorescence-labeled products were visualized by a Typhoon FLA 9500 (GE Healthcare) and quantified by ImageJ, version 1.5.3 (NIH). The extended primer fraction was calculated by dividing the amount of extended primer by the amount of primer added in reaction. The percent of extended primer was plotted against time and the data were fit to a single exponential equation:

$$[\text{product}] = A\text{x}\left(1 - e^{-k\text{obs}t}\right) \quad (1)$$

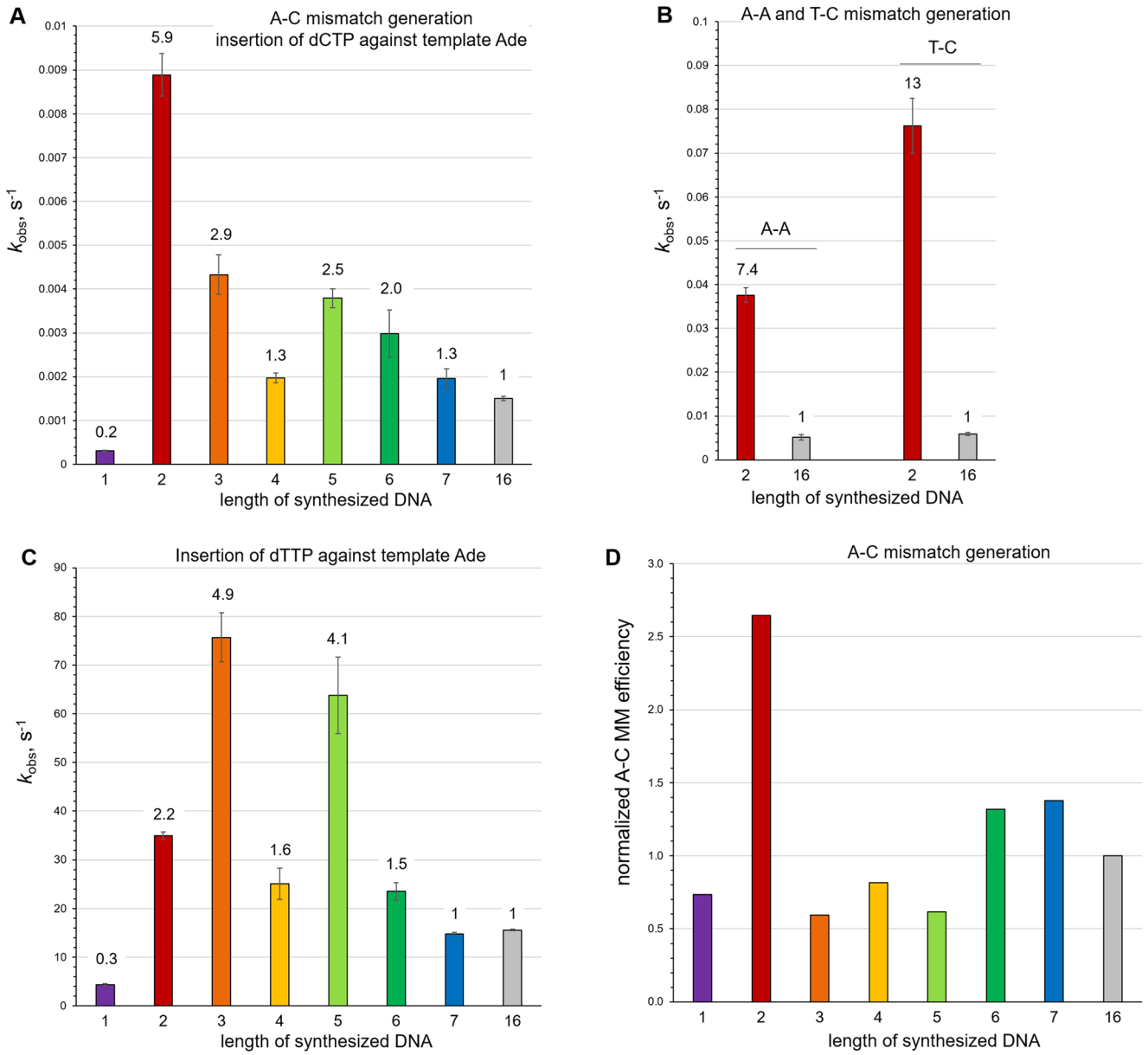

Figure 3. The length of a DNA track affects insertion rates of correct and incorrect dNMPs by hPolα at different levels. (**A**) The rate of A–C MM generation depends on the length of synthesized DNA. The numbers above the bars indicate the ratio of rates obtained for the corresponding primer and a DNA primer. (**B**) Formation of A–A and T–C MMs is significantly faster upon RNA primer extension with a second dNTP (dATP or dCTP, respectively) than on DNA. (**C**) The rates of cognate dTTP incorporation show spikes upon the third and fifth steps of DNA synthesis. (**D**) Polα shows the highest efficiency of A–C MM formation at the second step of DNA synthesis. For each primer, the rate of A–C MM formation was divided by the rate of cognate dTMP insertion and normalized to the value obtained for a DNA primer. For DNA synthesis steps one to eighth, the T1 template with annealed primers P2 to P8, respectively, was used. T1:P1 was used for sixteenth step.

where A is the amplitude, k_{obs} is the observed rate for dNTP incorporation and t is the time. The mean k_{obs} values and standard deviations were calculated from three independent experiments.

RESULTS AND DISCUSSION

To probe the Polα mutagenic potential during the early and late DNA elongation steps, we compared the rates of misinsertion and extension of mismatched duplexes using a chimeric RNA–DNA primer with two deoxynucleotides at the 3′-end as well as a 15-mer DNA primer, respectively (Supplemental Table S1). Reactions were conducted at single-turnover conditions in the presence of 3 μM Polα and 0.25 μM T:P, which were premixed before the reaction start, initiated by addition of catalytic Mg^{2+} ions and dNTP. It was found that misinsertion rates for A–C and T–C MMs are 3- to 4-fold higher in the case of a chimeric primer (Supplemental Figure S1). Moreover, the rates of extension of mismatched duplexes are 10-fold higher on a chimeric primer (Supplemental Figure S2). These results indicate that MM insertion and extension efficiencies are

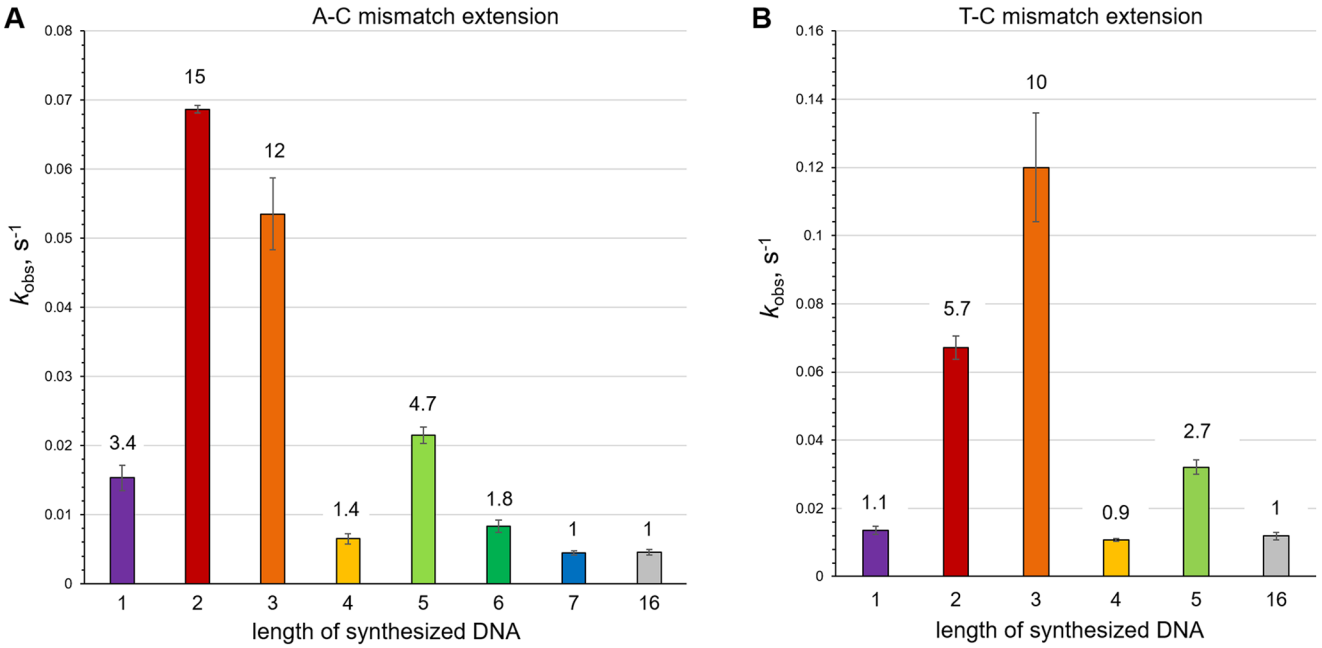

Figure 4. hPolα shows the increased rates of MM extension at the second, third, and fifth steps of DNA synthesis. (**A**) The rate of A–C MM extension depends on the length of synthesized DNA. The numbers above the bars indicate the ratio of rates obtained for the corresponding primer and a DNA primer. (**B**) The rates of T–C MM extension show spikes at the same DNA elongation steps as for A–C MM. For DNA synthesis steps one to eighth, the primers P2 to P8 were used, respectively; P1 was used for sixteenth step. Templates T4 and T5 were used in the case of A–C and T–C MM extension, respectively. All primers were extended with cognate dTTP.

highly dependent on primer structure, and Polα has an elevated mutagenic potential at the beginning of DNA primer synthesis.

In order to gather more information about Polα fidelity at each step of RNA primer extension, we analyzed the efficiency of A–C MM incorporation upon addition of the first through the sixth dNMPs. Upon attachment of the first dNMP to an RNA primer, Polα shows the lowest rate of A–C MM generation (Figure 3A). Previously, we observed this phenomenon for all 12 mismatches using a semi-quantitative assay (13). Interestingly, upon attachment of the second dNMP, there is a spike in misinsertion activity with an almost six-fold higher rate of A–C MM generation in comparison to a DNA primer (Figure 3A). Notably, the rate of A–C MM formation is 30-fold higher at the second versus the first step of an RNA primer extension with deoxynucleotides (Figure 3A). Similar to A–C MM, Polα shows 7.4- and 13-fold higher misinsertion rates of A–A and T–C MM generation, respectively, at the second versus the sixteenth DNA synthesis step (Figure 3B). Upon A–A MM formation, human primosome demonstrates comparable with Polα rates resulting in 5.3-fold difference between the same DNA synthesis steps (Supplemental Figure S3). This result indicate that the other primosome subunits do not affect the accuracy of DNA synthesis by Polα.

Next, we measured the rates of dTMP insertion opposite template Ade using the same primers. Surprisingly, the rate of correct nucleotide insertion also significantly varies during RNA extension with the first six deoxynucleotides (Figure 3C), but the activity spikes are distributed differently compared to A–C MM formation (compare panels A and C). The significant variation in the DNA polymerization rate at the early stage of DNA synthesis is likely due to the rigid T:P-binding cleft near the active site and primer bending by Polα at the fourth position from the 3′-end (13). A normalization of misinsertion rates revealed the highest efficiency of A–C MM formation upon the second dNMP insertion, with an almost three-fold bigger value in comparison to the late DNA elongation step (Figure 3D).

Analysis of A–C MM extension showed a more than 10-fold higher activity at the second and third steps of DNA elongation than on a DNA primer (Figure 4A). Interestingly, extension of A–C MM on the RNA primer is 3.4 times more efficient than on DNA. This might be important for efficient extension of MMs introduced by primase during RNA primer synthesis (25). Of note, Polα showed five-fold lower activity upon A–C MM generation on the RNA primer versus DNA (Figure 3A). Experiments with T–C MM extension also showed an activity spike at the second, third, and fifth steps of DNA synthesis (Figure 4B). Notably, upon extension of both MMs, A–C and T–C, Polα activity is at least 10-fold higher at the third step of RNA extension with DNA than on a DNA primer. This seems to be important for efficient extension of MMs introduced at the second step of DNA synthesis when Polα fidelity is compromised at most (Figure 3D).

Stability of the Polα/T:P complex is an important factor for MM extension because it defines the chances of a primer to be extended before the complex dissociates. In this regard, we analyzed hPolα interaction with DNA and RNA–DNA chimeric primers by using Octet K2, which employs the Bio-Layer Interferometry technology to monitor molecular interactions in real time. Pre-annealed template:primers with a biotin at the template 5′-end (Supple-

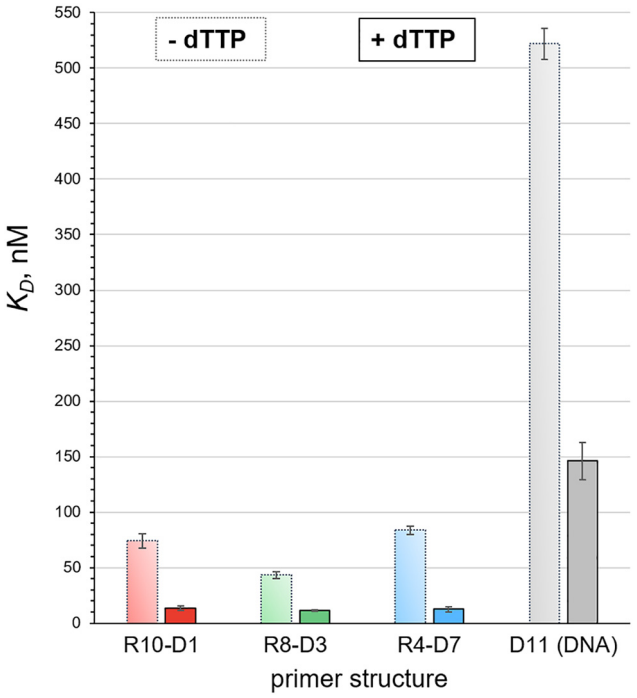

Figure 5. hPolα makes stronger interaction with chimeric primers than with a DNA primer. The corresponding k_{on}, k_{off} and K_D values are shown in Supplemental Table S2.

mental Table S1) were loaded on streptavidin biosensors and dipped into Polα solutions with different concentrations.

Analysis of Polα affinity to template:primers containing a DNA primer or chimeric RNA–DNA primers with one, three, and seven dNMPs at the 3′-end revealed an ∼10-fold stronger interaction with RNA-containing primers (Figure 5), which is mostly due to reduced k_{off} values (Supplemental Table S2). In line with our recent report about the effect of dNTP on Polα interaction with a DNA duplex (24), Polα/T:P complexes containing chimeric primers are significantly stabilized in the presence of cognate dTTP (Figure 5) and show similar K_D values in a range of 11.3–13.5 nM (Supplemental Table S2). These data revealed that the T:P binding site of hPolα is specific to chimeric primers. Notably, hPolε has a similar T:P binding site (26,27) but exhibits no selectivity toward RNA–DNA primers (28).

The results of initial binding studies (Figure 5) indicate that RNA-containing primers may stabilize the Polα/T:P complex in the presence of mismatches. In this regard, we analyzed the effect of different MMs on the stability of Polα/T:P complexes containing a DNA or a chimeric primer with three dNMPs at the 3′-end (Figure 6A and Table 1). To mimic MM at the insertion site of Polα, which must be occupied by a nascent base pair to allow DNA polymerization, we used dCTP or dGTP against template Thy or Ade. To mimic MM at the post-insertion site, which corresponds to incorrect dNMP insertion during the preceding DNA polymerization step, we used cognate dTTP and template:primers with a 3′-mispair T–C or A–C by replacing template Gua with Thy or Ade, respectively (Supplemental Table S1). These experiments have shown that the chimeric primer stabilizes the Polα/T:P complex in the presence of MMs (Figure 6A and Table 1). Depending on MM, the difference in K_D values for a chimeric and a DNA primer varies from several-fold to >10-fold.

Comparison of Polα interaction with chimeric primers containing seven and eight dNMPs showed a significant change in affinity either for cognate complexes or in the presence of MMs (Figure 6B and Supplemental Table S3). These data indicate that after RNA primer extension with eight dNMPs, Polα affinity to T:P gradually declines. This conclusion is consistent with structural studies showing that hPolα interacts with nine of the duplex bases of the template and with five of the duplex bases of the primer (13). Probably, the T:P-binding site of Polα is optimal for the double helix of a DNA:RNA duplex, which is wider than a DNA:DNA duplex.

Increased efficiency of dNTP insertion and stability of Polα/T:P complexes at the beginning of DNA primer synthesis makes the complexes more productive for MM extension. The probability of primer extension during the existence of the complex Polα/T:P depends on the rates of dNTP insertion and complex dissociation and defines the primer extension efficiency $f_{ext} = k_{obs}/(k_{obs} + k_{off})$. For example, for a Polα/T:P complex with a DNA duplex containing A–C MM, the rate of primer extension ($k_{obs} = 0.00457$ s^{-1}; Figure 4A) is 80 times lower in comparison to the rate of complex dissociation ($k_{off} = 0.364$ s^{-1}; Table 1), resulting in $f_{ext} = 0.012$. So, on average, ∼80 association/dissociation cycles of the Polα/DNA:DNA complex will take place before extension of A–C MM. This estimate indicates that the Polα complex with a mismatched DNA duplex is highly non-productive for the subsequent extension.

In contrast, the efficiency of A–C MM extension on a chimeric primer with three deoxynucleotides ($f_{ext} = 0.042$; the fourth step of DNA synthesis) is 3.5-fold higher than on a DNA primer, which is due to the increased rate of DNA polymerization ($k_{obs} = 0.0065$ s^{-1}; Figure 4A) and the reduced rate of complex dissociation ($k_{off} = 0.149$ s^{-1}; Table 1). Furthermore, a DNA polymerization rate is ∼10 times higher at the second and third DNA synthesis steps compared to the fourth step (Figure 4A), thus increasing f_{ext} several-fold.

These studies revealed significant mutagenic potential of hPolα at the first steps of DNA primer synthesis. This effect is dictated by the structure of a chimeric RNA–DNA primer and is based on increased Polα affinity to T:P and its DNA polymerization activity. Efficient MM extension on chimeric primers should prevent Polα and the replisome from stalling at the early DNA elongation stage, when it would be difficult to load the Polδ/PCNA complex on a 11–15 bp duplex (29) to allow Polδ to proofread MM and continue DNA synthesis. Moreover, a very inefficient RNA primer extension by Polδ (30) suggests that its ability to proofread MM on RNA-containing primers is also significantly compromised. Accordingly, a proposed mechanism of correction of Polα-introduced mistakes by Polδ (21) mainly applies to the late DNA elongation stage. Indeed, low efficiency of MM extension on a DNA primer, which results in Polα idling, would facilitate early loading of RFC/PCNA and then Polδ.

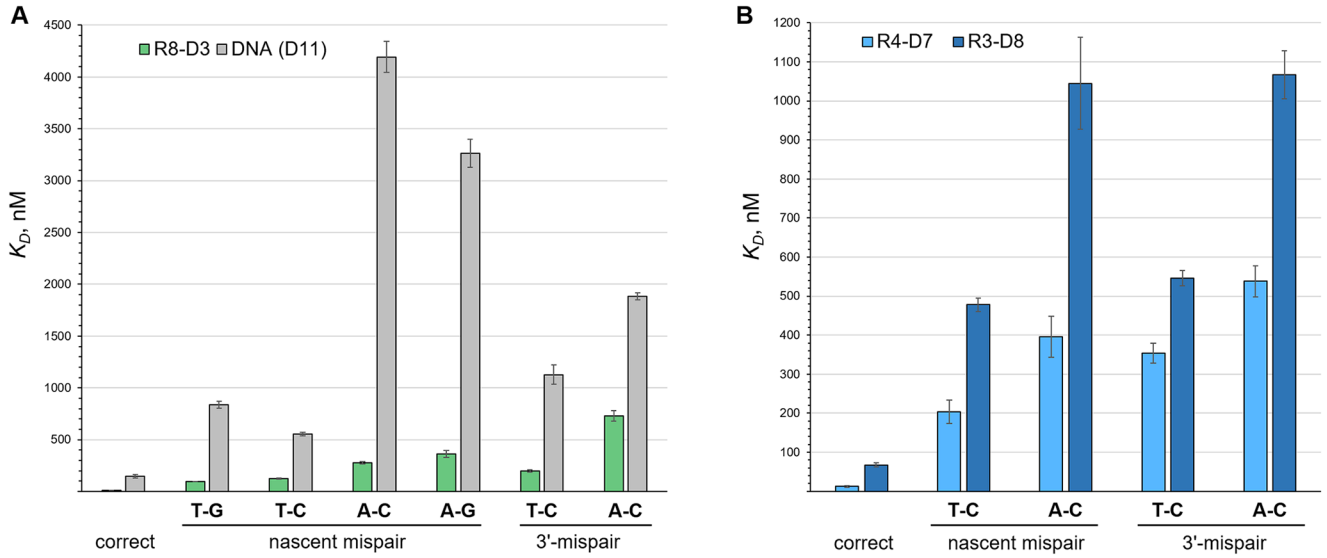

Figure 6. hPolα exhibits increased affinity to T:P with chimeric RNA–DNA primers in the presence of MMs. (**A**) In the presence of different MMs at the insertion and post-insertion sites, hPolα shows higher affinity to a chimeric primer. (**B**) hPolα interaction with chimeric primers significantly weakens after RNA primer extension with eighth dNMP. For panels A and B, the corresponding k_{on}, k_{off}, and K_D values are shown in Table 1 and Supplemental Table S3, respectively.

Table 1. Effect of mismatches and primer structure on Polα interaction with T:P

Primer	Template	dNTP	Nascent base/mis-pair	3′-base/mis-pair	K_D[a] nM	k_{on} mM^{-1} s^{-1}	k_{off} $\times 10^{-3}$ s^{-1}
P12 (R_8-D_3)	T6	dTTP	A–T	G–C	11.3 ± 0.69	288 ± 39	3.24 ± 0.24
	T9	dGTP	**T–G**	G–C	97.4 ± 1.3	255 ± 40	24.8 ± 3.6
	T9	dCTP	**T–C**	G–C	125 ± 3.7	254 ± 15	31.7 ± 0.92
	T6	dCTP	**A–C**	G–C	277 ± 11	299 ± 41	82.4 ± 7.6
	T6	dGTP	**A–G**	G–C	361 ± 33	240 ± 25	86.2 ± 1.3
	T7	dTTP	A–T	**T–C**	198 ± 9.2	276 ± 23	54.7 ± 7.0
	T8	dTTP	A–T	**A–C**	730 ± 51	204 ± 15	149 ± 21
P9 (DNA)	T6	dTTP	A–T	G–C	146 ± 17	272 ± 19	39.5 ± 1.8
	T9	dGTP	**T–G**	G–C	837 ± 35	218 ± 8.0	183 ± 14
	T9	dCTP	**T–C**	G–C	553 ± 18	196 ± 19	109 ± 6.9
	T6	dCTP	**A–C**	G–C	4194 ± 150	119 ± 8.2	498 ± 20
	T6	dGTP	**A–G**	G–C	3264 ± 136	134 ± 6.0	437 ± 16
	T7	dTTP	A–T	**T–C**	1127 ± 94	174 ± 11	196 ± 28
	T8	dTTP	A–T	**A–C**	1883 ± 33	193 ± 11	364 ± 28

[a] K_d values are obtained by dividing k_{off} by k_{on}.
Mispairs are in bold. Data are presented as mean ± SD ($n = 3$).

In the primase-Polα complex, the C-terminal domain of the primase accessory subunit ($p58_C$) is flexibly tethered to the rest of primosome and works as a processivity factor for Polα, by holding the 5′-end of an RNA primer when Polα extends the primer 3′-end with deoxynucleotides (4). Human Polα has low intrinsic processivity (13,31) and the $p58_C$/T:P interaction increases it, providing quick reloading of the Polα catalytic domain on T:P (4). The critical role in $p58_C$/primer interaction plays the triphosphate group located at the 5′-end of an RNA primer (32). This explains why the primosome demonstrates higher processivity of DNA synthesis on RNA polymerase- or primase-synthesized primers compared to the chemically synthesized primers containing no triphosphate (4,33).

Previously it was shown that increased processivity of DNA synthesis on primase-synthesized primers is mediated by a reduced rate of the primosome/T:P complex dissociation and not by changes in DNA polymerization rate (33). Similar to correct dNMP insertion, catalysis of MM formation and extension should not depend on primase interaction with the primer 5′-end. Accordingly, we propose that the described here effect of primer structure on Polα fidelity plays an important role *in vivo* upon elongation of primase-synthesized primers. Consistent with our findings, changing the primer from DNA to RNA significantly enhanced the ability of human Polα to bypass abasic lesions (34) and to tolerate arabinofuranosyl nucleotides (35).

The outcome of mutations introduced by Polα at the beginning of DNA synthesis needs further investigation. At the final step of Okazaki fragment synthesis, Polδ and flap endonuclease 1 (FEN1) work sequentially to remove an RNA primer located at the 5′-end of the preceding Okazaki fragment (36). In this iterative process termed nick-translation, Polδ inserts one nucleotide resulting in strand displacement and formation of a 1-nt flap, then Polδ hands off the flapped substrate to FEN1, which removes

5′-rNMP. When all ribonucleotides from the downstream strand are removed, DNA ligase 1 is able to seal the nick. According to structural data, human DNA ligase 1 has a relaxed binding site for the DNA strand synthesized by Polα (37). This suggests that DNA ligase 1 may not discriminate efficiently against MMs downstream of the nick, especially the ones that do not substantially disturb the DNA duplex, like T–G, T–C and A–C. There is an evidence for existence of a specific MutSa-dependent, MutLa-independent mismatch repair process called Polα-segment error editing (AEE) where Polα generated errors are excised by the FEN1/MSH2 complex (38).

DATA AVAILABILITY

The data that support the findings of this study are included in the Supplementary Data file or available from the corresponding author upon request.

SUPPLEMENTARY DATA

Supplementary Data are available at NAR Online.

ACKNOWLEDGEMENTS

We thank K. Jordan for editing this manuscript.
Author contributions: Conceptualization: A.G.B., T.H.T. Methodology: A.G.B. Investigation: A.E.L., A.G.B., L.M.M. Visualization: A.E.L., A.G.B., L.M.M., N.D.B., T.H.T. Funding acquisition: T.H.T. Project administration: N.D.B. Supervision: T.H.T. Writing – original draft: A.E.L., A.G.B. Writing – review & editing: A.G.B., T.H.T.

FUNDING

National Institute of General Medical Sciences [R35GM127085 to T.H.T.]. Funding for open access charge: National Institute of General Medical Sciences [R35GM127085].
Conflict of interest statement. None declared.

REFERENCES

1. Burgers,P.M.J. and Kunkel,T.A. (2017) Eukaryotic DNA replication fork. *Annu. Rev. Biochem.*, **86**, 417–438.
2. Pellegrini,L. and Costa,A. (2016) New insights into the mechanism of DNA duplication by the eukaryotic replisome. *Trends Biochem. Sci.*, **41**, 859–871.
3. Baranovskiy,A.G., Babayeva,N.D., Zhang,Y., Gu,J., Suwa,Y., Pavlov,Y.I. and Tahirov,T.H. (2016) Mechanism of concerted RNA–DNA primer synthesis by the human primosome. *J. Biol. Chem.*, **291**, 10006–10020.
4. Baranovskiy,A.G., Lisova,A.E., Morstadt,L.M., Babayeva,N.D. and Tahirov,T.H. (2022) Insight into RNA–DNA primer length counting by human primosome. *Nucleic Acids Res.*, **50**, 6264–6270.
5. Murakami,Y., Eki,T. and Hurwitz,J. (1992) Studies on the initiation of simian virus 40 replication in vitro: RNA primer synthesis and its elongation. *Proc. Natl. Acad. Sci. U.S.A.*, **89**, 952–956.
6. Yang,W., Lee,J.Y. and Nowotny,M. (2006) Making and breaking nucleic acids: two-Mg^{2+}-ion catalysis and substrate specificity. *Mol. Cell*, **22**, 5–13.
7. He,Q., Lin,X., Chavez,B.L., Agrawal,S., Lusk,B.L. and Lim,C.J. (2022) Structures of the human CST-Polalpha-primase complex bound to telomere templates. *Nature*, **608**, 826–832.
8. Zaug,A.J., Goodrich,K.J., Song,J.J., Sullivan,A.E. and Cech,T.R. (2022) Reconstitution of a telomeric replicon organized by CST. *Nature*, **608**, 819–825.
9. Cai,S.W., Zinder,J.C., Svetlov,V., Bush,M.W., Nudler,E., Walz,T. and de Lange,T. (2022) Cryo-EM structure of the human CST-Polalpha/primase complex in a recruitment state. *Nat. Struct. Mol. Biol.*, **29**, 813–819.
10. Mizuno,T., Hirabayashi,K., Miyazawa,S., Kobayashi,Y., Shoji,K., Kobayashi,M., Hanaoka,F., Imamoto,N. and Torigoe,H. (2021) The intrinsically disordered N-terminal region of mouse DNA polymerase alpha mediates its interaction with POT1a/b at telomeres. *Genes Cells*, **26**, 360–380.
11. Starokadomskyy,P., Gemelli,T., Rios,J.J., Xing,C., Wang,R.C., Li,H., Pokatayev,V., Dozmorov,I., Khan,S., Miyata,N. *et al.* (2016) DNA polymerase-alpha regulates the activation of type i interferons through cytosolic RNA:DNA synthesis. *Nat. Immunol.*, **17**, 495–504.
12. Han,T., Goralski,M., Capota,E., Padrick,S.B., Kim,J., Xie,Y. and Nijhawan,D. (2016) The antitumor toxin CD437 is a direct inhibitor of DNA polymerase alpha. *Nat. Chem. Biol.*, **12**, 511–515.
13. Baranovskiy,A.G., Duong,V.N., Babayeva,N.D., Zhang,Y., Pavlov,Y.I., Anderson,K.S. and Tahirov,T.H. (2018) Activity and fidelity of human DNA polymerase alpha depend on primer structure. *J. Biol. Chem.*, **293**, 6824–6843.
14. Makarova,A.V. and Burgers,P.M. (2015) Eukaryotic DNA polymerase zeta. *DNA Repair (Amst.)*, **29**, 47–55.
15. Pavlov,Y.I., Shcherbakova,P.V. and Rogozin,I.B. (2006) Roles of DNA polymerases in replication, repair, and recombination in eukaryotes. *Int. Rev. Cytol.*, **255**, 41–132.
16. Reijns,M.A.M., Kemp,H., Ding,J., de Proce,S.M., Jackson,A.P. and Taylor,M.S. (2015) Lagging-strand replication shapes the mutational landscape of the genome. *Nature*, **518**, 502–506.
17. Mendelman,L.V., Petruska,J. and Goodman,M.F. (1990) Base mispair extension kinetics. Comparison of DNA polymerase alpha and reverse transcriptase. *J. Biol. Chem.*, **265**, 2338–2346.
18. Perrino,F.W. and Loeb,L.A. (1989) Differential extension of 3′ mispairs is a major contribution to the high fidelity of calf thymus DNA polymerase-alpha. *J. Biol. Chem.*, **264**, 2898–2905.
19. Copeland,W.C., Lam,N.K. and Wang,T.S. (1993) Fidelity studies of the human DNA polymerase alpha. The most conserved region among alpha-like DNA polymerases is responsible for metal-induced infidelity in DNA synthesis. *J. Biol. Chem.*, **268**, 11041–11049.
20. Tanaka,S., Cao,K., Niimi,A., Limsirichaikul,S., Miao,H.Q., Nakamura,N., Murate,T., Hasegawa,Y., Takahashi,T. and Suzuki,M. (2010) Functions of base selection step in human DNA polymerase alpha. *DNA Repair (Amst.)*, **9**, 534–541.
21. Pavlov,Y.I., Frahm,C., Nick McElhinny,S.A., Niimi,A., Suzuki,M. and Kunkel,T.A. (2006) Evidence that errors made by DNA polymerase alpha are corrected by DNA polymerase delta. *Curr. Biol.*, **16**, 202–207.
22. Kunkel,T.A., Roberts,J.D. and Sugino,A. (1991) The fidelity of DNA synthesis by the catalytic subunit of yeast DNA polymerase alpha alone and with accessory proteins. *Mutat. Res.*, **250**, 175–182.
23. Zhang,Y., Baranovskiy,A.G., Tahirov,T.H. and Pavlov,Y.I. (2014) The C-terminal domain of the DNA polymerase catalytic subunit regulates the primase and polymerase activities of the human DNA polymerase alpha-primase complex. *J. Biol. Chem.*, **289**, 22021–22034.
24. Baranovskiy,A.G., Babayeva,N.D., Lisova,A.E., Morstadt,L.M. and Tahirov,T.H. (2022) Structural and functional insight into mismatch extension by human DNA polymerase alpha. *Proc. Natl. Acad. Sci. U.S.A.*, **119**, e2111744119.
25. Sheaff,R.J. and Kuchta,R.D. (1994) Misincorporation of nucleotides by calf thymus DNA primase and elongation of primers containing multiple noncognate nucleotides by DNA polymerase alpha. *J. Biol. Chem.*, **269**, 19225–19231.
26. Hogg,M., Osterman,P., Bylund,G.O., Ganai,R.A., Lundstrom,E.B., Sauer-Eriksson,A.E. and Johansson,E. (2014) Structural basis for processive DNA synthesis by yeast DNA polymerase varepsilon. *Nat. Struct. Mol. Biol.*, **21**, 49–55.
27. Jain,R., Rajashankar,K.R., Buku,A., Johnson,R.E., Prakash,L., Prakash,S. and Aggarwal,A.K. (2014) Crystal structure of yeast DNA polymerase epsilon catalytic domain. *PLoS One*, **9**, e94835.
28. Lisova,A.E., Baranovskiy,A.G., Morstadt,L.M., Babayeva,N.D. and Tahirov,T.H. (2022) Efficient discrimination against RNA-containing primers by human DNA polymerase epsilon. *Sci. Rep.*, **12**, 10163.

29. Lancey,C., Tehseen,M., Raducanu,V.S., Rashid,F., Merino,N., Ragan,T.J., Savva,C.G., Zaher,M.S., Shirbini,A., Blanco,F.J. *et al.* (2020) Structure of the processive human pol delta holoenzyme. *Nat. Commun.*, **11**, 1109.
30. Lee,S.H., Eki,T. and Hurwitz,J. (1989) Synthesis of DNA containing the simian virus 40 origin of replication by the combined action of DNA polymerases alpha and delta. *Proc. Natl. Acad. Sci. U.S.A.*, **86**, 7361–7365.
31. Copeland,W.C. and Wang,T.S. (1993) Mutational analysis of the human DNA polymerase alpha. The most conserved region in alpha-like DNA polymerases is involved in metal-specific catalysis. *J. Biol. Chem.*, **268**, 11028–11040.
32. Baranovskiy,A.G., Zhang,Y., Suwa,Y., Gu,J., Babayeva,N.D., Pavlov,Y.I. and Tahirov,T.H. (2016) Insight into the human DNA primase interaction with template-primer. *J. Biol. Chem.*, **291**, 4793–4802.
33. Thompson,H.C., Sheaff,R.J. and Kuchta,R.D. (1995) Interactions of calf thymus DNA polymerase alpha with primer/templates. *Nucleic Acids Res.*, **23**, 4109–4115.
34. Zerbe,L.K., Goodman,M.F., Efrati,E. and Kuchta,R.D. (1999) Abasic template lesions are strong chain terminators for DNA primase but not for DNA polymerase alpha during the synthesis of new DNA strands. *Biochemistry*, **38**, 12908–12914.
35. Kuchta,R.D., Ilsley,D., Kravig,K.D., Schubert,S. and Harris,B. (1992) Inhibition of DNA primase and polymerase alpha by arabinofuranosylnucleoside triphosphates and related compounds. *Biochemistry*, **31**, 4720–4728.
36. Stodola,J.L. and Burgers,P.M. (2016) Resolving individual steps of Okazaki-fragment maturation at a millisecond timescale. *Nat. Struct. Mol. Biol.*, **23**, 402–408.
37. Pascal,J.M., O'Brien,P.J., Tomkinson,A.E. and Ellenberger,T. (2004) Human DNA ligase i completely encircles and partially unwinds nicked DNA. *Nature*, **432**, 473–478.
38. Liu,S., Lu,G., Ali,S., Liu,W., Zheng,L., Dai,H., Li,H., Xu,H., Hua,Y., Zhou,Y. *et al.* (2015) Okazaki fragment maturation involves alpha-segment error editing by the mammalian FEN1/MutSalpha functional complex. *EMBO J.*, **34**, 1829–1843.